Volume 24, No 4 | International Journal of Radiation Research, October 2026

CDCA7 as a novel biomarker beside imaging to predict prognosis and tumor immunity in glioma patients

G. Zhu[1#], K. Chen[1#], S. Yang[2], P. Feng[1], W. Fan[1], Y. Peng[1], J. Wei[1], X. Gao[1*]

[1]*Department of Neurosurgery, The Second Affiliated Hospital of Jiujiang University, Jiujiang, China*
[2]*Department of Neurosurgery, The Affiliated Hospital of Jiujiang University, Jiujiang, China*

► ***Original article***

***Corresponding author:**
Xiang Gao, M.D.,
***E-mail:** soar7974@163.com*

Received: June 2026
Final revised: August 2026
Accepted: August 2026

Int. J. Radiat. Res., October 2026; 24(4): 1197-1205

DOI: 10.61186/ijrr.24.4.34

Keywords: *Glioma, magnetic resonance imaging, radiomics, CDCA7, prognosis.*

[#]These authors contributed equally to this work.

ABSTRACT

Background: Cell division cycle-associated 7 (CDCA7) is implicated in tumor proliferation, but its clinical, immune, and imaging relevance in glioma remains incompletely defined. ***Materials and Methods:*** CDCA7 expression and prognostic value were evaluated using TCGA/GTEx, CGGA, GEO, and CCLE datasets. Immune-cell infiltration, immune checkpoints, and predicted immune-checkpoint blockade response were assessed using ssGSEA, TIMER, and TIDE. LinkedOmics-based co-expression, Gene Ontology, KEGG, and GSEA analyses were performed. Preoperative MRI features were analyzed in 286 patients with matched TCGA transcriptomic and TCIA imaging data, and radiomic features were evaluated in a subset of 85 patients. CDCA7 expression was validated in clinical tissues, and loss-of-function experiments were conducted in U251 and T98G cells. ***Results:*** CDCA7 was significantly overexpressed in glioma and increased with tumor grade. High CDCA7 expression was associated with poorer overall, disease-specific, and progression-free survival and showed strong diagnostic performance (AUC = 0.982). CDCA7-high tumors more frequently demonstrated contrast enhancement, necrosis, severe edema, multifocality, and larger contrast-enhancing volumes. After adjustment for age, IDH status, and histological grade, necrosis (adjusted OR = 2.32), contrast enhancement (adjusted OR = 1.85), and severe edema (adjusted OR = 2.45) remained independently associated with high CDCA7 expression. A five-feature radiomic model predicted CDCA7 status with an AUC of 0.76. CDCA7 expression correlated with immune infiltration and checkpoint molecules. CDCA7 knockdown reduced proliferation, migration, and invasion and increased sensitivity to temozolomide and cisplatin. ***Conclusion:*** CDCA7 is a prognostic, immune-related, and imaging-associated biomarker in glioma and may represent a potential therapeutic target.

INTRODUCTION

Gliomas are the most common and aggressive tumors of the central nervous system [1]. The World Health Organization classifies Grade II and III gliomas as diffuse low-grade gliomas, with 5-year survival rates of approximately 50% and 30%, respectively [2]. Patients diagnosed with high-grade gliomas (WHO grades III and IV) face a significantly poor prognosis, with the median survival for grade IV gliomas being 16.0 months, ranging from 9.3 to 27.5 months [3]. Gliomas are marked by rapid growth, increased infiltration and difficulty of surgical removal The rapid growth of gliomas, extensive invasion and high infiltration make its surgical removal difficult. Although treatment strategies have been improved by neuro-microsurgical methods, immunotherapy and gene therapy, glioma patients still suffer from high recurrence and mortality and low long-term survival rates. More in-depth studies are still needed on the molecular pathways and immune mechanisms of glioma progression, so as to improve therapeutic strategies [4-6].

For the diagnosis and monitoring of gliomas, conventional imaging methods continue to rely on computed tomography (CT) and magnetic resonance imaging (MRI) [7]. Nevertheless, these methods are constrained by their incapacity to predict molecular subtypes, response to immunotherapy, and differentiate tumor progression from treatment-related alterations. A paradigm shifts toward precision neuro-oncology through the integration of imaging data and molecular biomarkers [8]. The accuracy of glioma diagnosis and treatment has increased with the development of bioinformatic research, which has led to the inclusion of molecular biomarkers such as isocitrate dehydrogenase mutations in diagnostic guidelines [9]. Molecular markers combined with imaging features may enhance prognosis stratification, treatment decision making, and diagnostic precision.

Cell cycle regulation is significantly influenced by *CDCA7*, a direct target gene of c-Myc [10]. In many forms of cancer, it is essential for promoting cell invasion, proliferation, and metastasis. In ovarian cancer, *CDCA7* suppresses angiogenesis and cell cycle

[Downloaded from ijrr.com on 2026-11-12]

[DOI: 10.61186/ijrr.24.4.34]

progression by blocking enhancer of zeste homolog 2 [11]. In lung adenocarcinoma, *CDCA7* controls the cell cycle to promote tumor growth [12], and in esophageal squamous cell carcinoma, it promotes the TGF-β-induced epithelial-mesenchymal transition via influencing Smad4/Smad7 transcription [13]. Additionally, *CDCA7* has been identified as a possible prognostic and diagnostic marker for gastric and liver malignancies [14]. Additionally, it promotes tumor growth by controlling *CCNA2* expression in esophageal squamous cell carcinoma (ESCC) and mediating inflammatory apoptosis in gastric adenocarcinoma through the *TLR4*/NF-κB signaling pathway [15, 16]. Its role in glioma is still poorly understood, indicating the need for more investigation into its immune-related and carcinogenic properties [17, 18]. In this work, we investigated the novel role of *CDCA7* in tumor immunity, particularly its role in immune cell infiltration, which may provide new insights for therapeutic interventions, and its prognostic significance in gliomas. Furthermore, we suggest that *CDCA7* expression in conjunction with conventional imaging could function as a more complete biomarker for glioma treatment.

The multifaceted assessment of the molecular, imaging-associated, immune-related, and functional biomarker *CDCA7* in gliomas is new. In addition, we verified the expression and prognostic significance of *CDCA7* in many independent transcriptome datasets and investigated the relationship between *CDCA7* expression and preoperative MRI characteristics in individuals whose TCGA transcriptomic and TCIA imaging data matched. We also assessed radiomic features' capacity to predict *CDCA7* expression noninvasively. Immune-cell infiltration, immune-checkpoint expression, predicted immunotherapy response, co-expression networks, and enriched biological pathways were all incorporated into these imaging analyses. Finally, clinical tissue validation and *CDCA7* loss-of-function tests were used to examine the impact of *CDCA7* on glioma-cell proliferation, migration, invasion, apoptosis, and temozolomide and cisplatin sensitivity. Compared to gene expression and survival analysis alone, the integrated radiogenomic, immunological, bioinformatic, and experimental framework provides a more thorough assessment of *CDCA7*, indicating its potential involvement in glioma stratification and treatment development.

In this work, we investigated *CDCA7* in gliomas using both bioinformatic and experimental methods. Using publically accessible datasets from TCGA/GTEx, CGGA, GEO, and CCLE, *CDCA7* expression was described and its diagnostic and prognostic importance assessed. Additionally, we looked into the relationships between *CDCA7* expression and immune-cell infiltration, immune-checkpoint molecules, anticipated immunotherapy response, and biological pathways that are functionally enriched. Following the confirmation of *CDCA7* expression in clinical tissue samples, loss-of-function studies were conducted in glioma cell lines to investigate its roles in cell migration, invasion, proliferation, apoptosis, and sensitivity to cisplatin and temozolomide. Our combined strategy aimed to clarify the biology and clinical importance of *CDCA7* and investigate its potential as a therapeutic target and prognostic biomarker in gliomas.

MATERIALS AND METHODS

Study design and data sources

This unified bioinformatic and radiogenomic analysis was conducted to examine the expression, diagnostic and prognostic implications, immune interactions, biological functions, and links to magnetic resonance imaging attributes of *CDCA7* in glioma. Data on gene expression and clinical parameters were acquired from The Cancer Genome Atlas (TCGA), Genotype-Tissue Expression project (GTEx), Chinese Glioma Genome Atlas (CGGA), Gene Expression Omnibus (GEO), and Cancer Cell Line Encyclopedia (CCLE).

The TCGA-GTEx collection included 699 primary glioma samples alongside 1,157 normal brain tissues. The validation of the model externally involved three distinct GEO datasets, namely GSE16011 (comprising 276 glioma samples and 8 normal brain samples), GSE42656 (consisting of 65 brain tumor samples and 8 normal brain samples), and GSE66354 (including 136 brain tumor samples and 13 normal brain samples). *CDCA7* levels in glioma cell lines were analyzed inside the CCLE dataset. The entirety of the analyses was executed with R software version 4.3.3.

CDCA7 expression analysis

Gene expression matrices along with clinical data were retrieved from the relevant databases. The expression values of *CDCA7* were converted and standardized according to the processing protocols of each dataset. The differential expression between glioma and normal brain tissues was examined using the limma, DESeq2, or edgeR programs based on the data format. For subsequent studies, the glioma specimens were categorized into *CDCA7*-high and *CDCA7*-low cohorts using the median *CDCA7* expression level as the predetermined threshold. The two groups were compared using an independent-samples t-test when normality was satisfied and the Mann-Whitney U test when the data exhibited non-normal distribution.

Diagnostic and prognostic analyses

The ability of *CDCA7* to distinguish glioblastoma from healthy brain tissue was evaluated by receiver operating characteristic curves. The diagnostic

[Downloaded from ijrr.com on 2026-11-12]

[DOI: 10.61186/ijrr.24.4.34]

precision was measured by the area beneath the curve and its 95% confidence interval. The Kaplan-Meier survival curves were utilized to assess overall survival, disease-specific survival, and progression-free interval. Patients were categorized according to median *CDCA7* expression, and survival distributions were analyzed using the log-rank test. We assessed the capacity of *CDCA7* expression to forecast survival at 1, 5, and 10 years through time-dependent receiver operating characteristic analysis. Cox proportional-hazards regression models, both univariable and multivariable, were conducted to assess the independent relationship between *CDCA7* expression and patient survival. Clinicopathological factors such as age, gender, WHO grade, *IDH* mutation status, and 1p/19q codeletion status were evaluated as covariates. We presented hazard ratios together with 95% confidence intervals. A predictive nomogram was developed utilizing *CDCA7* expression alongside clinically relevant factors, employing the rms program. The model's calibration was evaluated by juxtaposing the survival probabilities predicted by the nomogram with the actual survival probabilities at 1, 5, and 10 years.

Acquisition of matched transcriptomic and MRI data

Preoperative MRI scans were retrieved from The Cancer Imaging Archive for patients with accessible transcriptomic and clinical information in the TCGA lower-grade glioma and glioblastoma initiatives. Patient identities were correlated between TCGA and TCIA on an individual patient basis. We omitted instances where the MRI assessments were devoid of comprehensive DICOM data, exhibited significant motion artifacts, were missing critical imaging sequences, or lacked *CDCA7* expression information. Following these criteria, we incorporated 286 patients possessing both transcriptomic and imaging information. *CDCA7* mRNA expression was expressed as log base 2 of (FPKM + 1). The median value of the expression was 4.22. Patients were categorized into *CDCA7*-high and *CDCA7*-low cohorts, with 143 individuals in each cohort.

Qualitative MRI assessment

Preoperative MRI assessments comprised precontrast T1-weighted, T2-weighted, fluid-attenuated inversion recovery, and postcontrast T1-weighted sequences. All assessments were autonomously evaluated by two neuroradiologists who were unaware of *CDCA7* expression and further molecular information. The subsequent qualitative MRI features were assessed:

1. Existence or nonexistence of contrast enhancement.
2. Existence or nonexistence of intratumoral necrosis.
3. Peritumoral edema categorized as absent/minimal, moderate, or pronounced.
4. Unilateral versus multifocal or multicentric pathology.
5. Anterior compared to non-anterior tumor positioning.

The assessment of interobserver concordance was conducted utilizing Cohen's κ coefficient. Conflicts between the two readers were settled via consensus evaluation.

Contrast-enhancing tumor volumetry

Contrast-enhancing tumor volume was segmented on postcontrast T1-weighted images with 3D Slicer version 5.0.3. Segmentation was semi-automatically performed with manual correction of lesions with poorly defined margins. Volume of interest for contrast enhancement was measured in cm3. In case of skewed distribution of the values, tumor-volume measurements were log-transformed for parametric analysis. Differences in contrast-enhancing tumor volume between *CDCA7*-high and *CDCA7*-low groups were analyzed using the Mann-Whitney U test.

Radiomic feature extraction and modelling

A radiomic subanalysis was performed on 85 patients with high-quality tumor delineations. Radiomic characteristics were derived from post-contrast T1-weighted and T2-FLAIR images utilizing PyRadiomics. A comprehensive assessment was conducted on 107 characteristics, encompassing first-order intensity, shape, gray-level co-occurrence matrix, gray-level run-length matrix, and gray-level size-zone matrix features. The association between ongoing *CDCA7* expression and individual radiomic characteristics was evaluated by Spearman correlation analysis. P values were modified for multiple comparisons via the Benjamini–Hochberg false-discovery-rate method, with an adjusted P value of less than 0.05 deemed significant. A radiomic model comprising five features was created to categorize individuals into *CDCA7*-high and *CDCA7*-low classifications. Model discrimination was assessed through leave-one-out cross-validation, and the results were expressed as the area under the receiver operating characteristic curve with a 95% confidence interval.

Association between MRI features and CDCA7 expression

The categorical MRI features were analyzed between the *CDCA7*-high and *CDCA7*-low cohorts utilizing Pearson's χ^2 test. The Cochran-Armitage trend test was employed to evaluate the sequential correlation between *CDCA7* expression categories and the severity of edema. Univariable logistic regression was conducted for every clinical and MRI variable. Clinically pertinent variables or those linked to *CDCA7* status identified in univariable analysis were incorporated into a multivariable logistic

[Downloaded from ijrr.com on 2026-11-12]

[DOI: 10.61186/ijrr.24.4.34]

regression model. The ultimate model assessed the independent relationships of necrosis, contrast enhancement, edema severity, and contrast-enhancing tumor volume with elevated *CDCA7* expression, controlling for age, *IDH* mutation status, and histological grade. Outcomes were presented as odds ratios accompanied by 95% confidence intervals. The c-statistic was employed to assess model discrimination.

Immune-cell infiltration analysis

The correlation between *CDCA7* expression and immune cell infiltration was assessed by single-sample gene-set enrichment analysis. Enrichment scores were computed for 24 immune cell populations, and their correlations with continuous *CDCA7* expression were evaluated through Spearman correlation analysis. The TIMER database was also employed to examine correlations between *CDCA7* expression and immune cells infiltrating tumors. Analyses and visualizations were conducted utilizing the ggplot2, ggpubr, ggExtra, limma, heatmap, reshape2, estimate, and immuneeconv packages.

Immune-checkpoint and immunotherapy-response analyses

The expression levels of immune-checkpoint genes such as *CD274*, *CTLA4*, *HAVCR2*, *LAG3*, *PDCD1*, *PDCD1LG2*, *SIGLEC15*, and *TIGIT* were analyzed in relation to *CDCA7*-high and *CDCA7*-low gliomas. The Tumor Immune Dysfunction and Exclusion algorithm was employed to assess the possible reaction to immune-checkpoint blocking. TIDE scores were analyzed across different *CDCA7* expression cohorts to investigate the correlation between *CDCA7* and anticipated immune evasion or responsiveness to immunotherapy.

Drug-sensitivity prediction

Associations between *CDCA7* expression and predicted drug sensitivity were evaluated using estimated half-maximal inhibitory concentration values. Spearman correlation analysis was used to assess the relationship between *CDCA7* expression and the predicted sensitivity to temozolomide, cisplatin, and other evaluated anticancer agents.

Co-expression and functional-enrichment analyses

LinkedOmics was used to identify genes co-expressed with *CDCA7* in 371 samples from the TCGA glioma cohort. Genes showing the strongest positive and negative correlations with *CDCA7* were displayed using volcano plots and heatmaps. Gene-set enrichment analysis was subsequently performed to identify biological functions and pathways related to *CDCA7*. Gene Ontology analysis included biological process, cellular component, and molecular function categories. Kyoto Encyclopedia of Genes and Genomes pathway analysis was performed to identify significantly enriched signaling and metabolic pathways.

Statistical analysis

Continuous variables were evaluated for normal distribution utilizing the Shapiro-Wilk test. Variables that follow a normal distribution are expressed as mean ± standard deviation and analyzed using the independent-samples t-test. Variables that do not follow a normal distribution are expressed as median and interquartile range, and were analyzed using the Mann-Whitney U test. Categorical variables are displayed as frequencies and percentages and were analyzed using Pearson's χ^2 test or a suitable trend test. The relationships were evaluated with Spearman's correlation coefficient. The Benjamini-Hochberg method was utilized for multiple-testing correction, assessing various radiomic or molecular characteristics. All statistical analyses were conducted as two-tailed tests, with a significance threshold set at $P<0.05$.

RESULTS

CDCA7 expression in pan-cancer datasets, glioma tissues, and glioma cell lines

Pan-cancer analysis of the TCGA–GTEx dataset showed that *CDCA7* expression was significantly elevated in 26 of 33 evaluated cancer types compared with the corresponding normal tissues. In the combined TCGA–GTEx glioma cohort, *CDCA7* expression was markedly higher in glioma tissues than in normal brain tissues (figure 1A). Independent datasets confirmed this pattern: *CDCA7* expression increased progressively with WHO grade in the CGGA cohort, and expression was significantly higher in glioma than in normal brain tissue in GSE16011, GSE42656, and GSE66354. In the 699-patient glioma cohort, *CDCA7* expression also increased significantly from WHO grade II to grades III and IV (all $P<0.001$; figure 1B).

CCLE analysis demonstrated detectable *CDCA7* expression across multiple glioma cell lines, with relatively high expression in T98G and CCF-STTG1 cells. Because this analysis was descriptive and did not include a predefined comparison group, no inferential P value was calculated.

Clinical tissue validation produced concordant findings. RT-qPCR demonstrated significantly higher *CDCA7* mRNA expression in glioma tissues than in non-neoplastic brain tissues (figure 1C), and western blotting showed greater *CDCA7* protein abundance in the three glioma specimens than in the three normal brain specimens (figure 1D).

Diagnostic and prognostic significance of CDCA7 in glioma

CDCA7 distinguished glioma tissues from healthy brain tissues with an area under the receiver operating characteristic curve of 0.982 (95% CI, 0.977

[Downloaded from ijrr.com on 2026-11-12]

[DOI: 10.61186/ijrr.24.4.34]

–0.988; figure 2A). Time-dependent ROC analysis yielded AUC values of 0.736, 0.742, and 0.582 for predicting overall survival at 1, 5, and 10 years, respectively. A nomogram incorporating *CDCA7* expression, WHO grade, *IDH* status, age, sex, and 1p/19q codeletion status showed close agreement between predicted and observed survival probabilities in the calibration analysis.

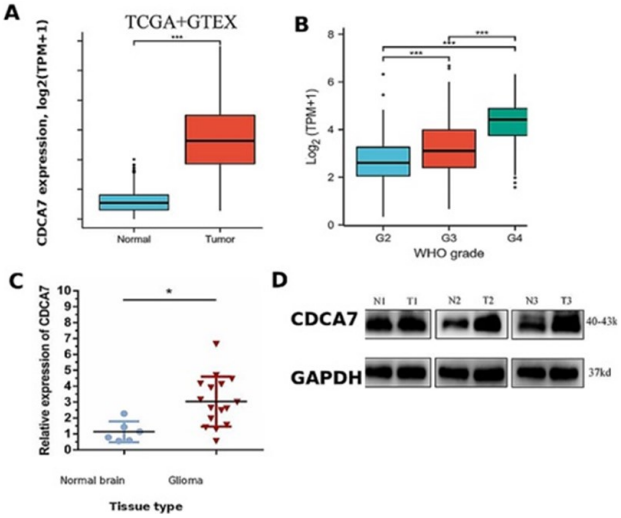


Figure 1. CDCA7 expression and validation in glioma. **(A)** CDCA7 expression in the combined TCGA–GTEx glioma and normal-brain cohorts. **(B)** CDCA7 expression across WHO grades II–IV. (C) RT-qPCR validation in 6 non-neoplastic brain tissues and 16 glioma tissues; the x-axis indicates tissue type and the y-axis indicates relative CDCA7 mRNA expression. **(D)** Western blot validation in 3 normal and 3 glioma tissues.

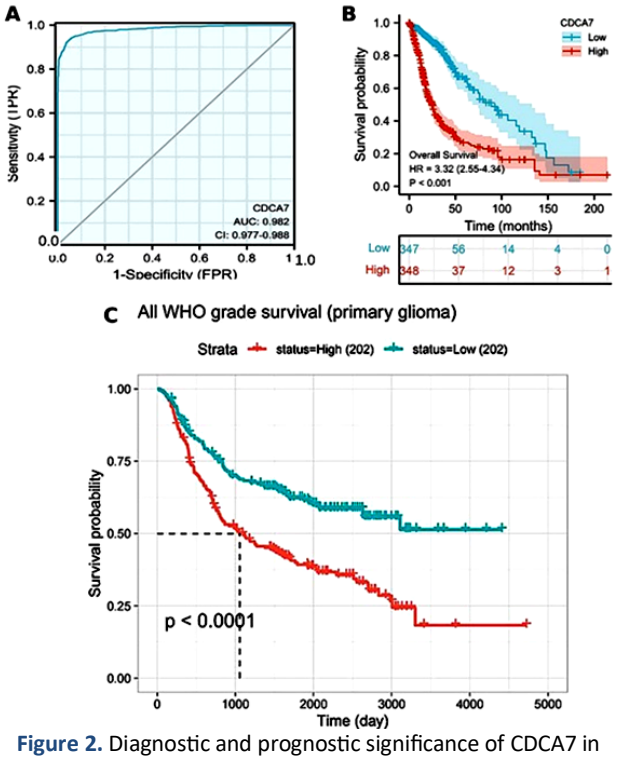


Figure 2. Diagnostic and prognostic significance of CDCA7 in glioma. **(A)** Receiver operating characteristic curve for distinguishing glioma from normal brain tissue. **(B)** Kaplan-Meier overall-survival analysis in the TCGA cohort. **(C)** Overall-survival validation in the CGGA cohort.

Kaplan-Meier analysis consistently associated high *CDCA7* expression with adverse outcomes. Patients with high *CDCA7* expression had significantly poorer overall survival than those with low expression (HR=3.32, 95% CI 2.55-4.34, P<0.001; figure 2B), as well as poorer disease-specific survival (HR=3.44, 95% CI 2.59-4.57, P<0.001) and a shorter progression-free interval (HR=2.54, 95% CI 2.04-3.18, P<0.001). The adverse association with overall survival was independently validated in the CGGA cohort (P<0.0001; figure 2C). Collectively, these findings link increased *CDCA7* expression to advanced glioma and poor prognosis.

Association between CDCA7 expression and MRI features in patients with glioma

After matching TCGA-LGG and TCGA-GBM transcriptomic data with curated preoperative MRI data from TCIA, 286 patients with complete imaging and RNA-sequencing data were included. *CDCA7* mRNA expression, expressed as log2(FPKM+1), had a median value of 4.22 (IQR, 3.18–5.41). Patients were dichotomized at the median into *CDCA7*-high and *CDCA7*-low groups, with 143 patients in each group.

Patients in the *CDCA7*-high group were older than those in the *CDCA7*-low group (56.9±13.7 versus 49.5±14.1 years) and were more frequently *IDH*-wildtype (82.5% versus 45.3%) and histologically classified as glioblastoma (66.4% versus 32.8%). In contrast, 1p/19q codeletion (8.4% versus 24.3%) and *MGMT* promoter methylation (37.8% versus 52.6%) were less frequent in the *CDCA7*-high group. Sex distribution did not differ significantly between groups.

The two neuroradiologists achieved substantial-to-almost-perfect agreement for the evaluated MRI features. *CDCA7*-high tumors displayed a more aggressive imaging phenotype: contrast enhancement was present in 85.2% versus 62.4%, intratumoral necrosis in 73.1% versus 44.8%, severe edema in 38.7% versus 24.8%, and multifocal or multicentric disease in 28.9% versus 18.2% of *CDCA7*-high and *CDCA7*-low tumors, respectively. Tumor location did not differ significantly between groups. Median contrast-enhancing tumor volume was also greater in the *CDCA7*-high group (54.2 cm^3 [IQR, 28.7–89.5] versus 36.8 cm^3 [IQR, 18.2–67.4]; table 1).

Table 1. MRI features stratified by CDCA7 expression.

MRI feature	*CDCA7*-low (n=143)	*CDCA7*-high (n=143)	*P* value
Contrast enhancement, n (%)	89 (62.4)	122 (85.2)	<0.001
Necrosis, n (%)	64 (44.8)	105 (73.1)	<0.001
Edema severity, n (%)			<0.001*
None/Mild	59 (41.6)	32 (22.4)	
Moderate	48 (33.6)	56 (38.9)	
Severe	36 (24.8)	55 (38.7)	
Multifocality, n (%)	26 (18.2)	41 (28.9)	0.032
CE-VOI (cm^3), median (IQR)	36.8 (18.2-67.4)	54.2 (28.7-89.5)	0.002‡

*Cochran-Armitage trend test; ‡Mann-Whitney U test. CE-VOI = contrast-enhancing volume of interest.

[Downloaded from ijrr.com on 2026-11-12]

[DOI: 10.61186/ijrr.24.4.34]

In univariable logistic regression, contrast enhancement (OR=3.43, 95% CI 2.02–5.83, P<0.001), necrosis (OR=3.33, 95% CI 2.05–5.42, P<0.001), severe edema versus none or mild edema (OR=2.78, 95% CI 1.56–4.95, P<0.001), and each doubling of contrast-enhancing tumor volume (OR=1.34, 95% CI 1.10–1.63, P=0.004) were associated with high *CDCA7* expression. After adjustment for age, *IDH* mutation status, and histological grade, necrosis (adjusted OR=2.32, 95% CI 1.39–3.87, P=0.001), contrast enhancement (adjusted OR=1.85, 95% CI 1.08–3.17, P=0.025), and severe edema (adjusted OR=2.45, 95% CI 1.32–4.55, P=0.004) remained independently associated with high *CDCA7* expression. Contrast-enhancing tumor volume was no longer significant after adjustment (adjusted OR=1.12, 95% CI 0.95–1.33, P=0.18). The final model had a c-statistic of 0.782 (table 2).

Table 2. Multivariable logistic regression for high *CDCA7* expression.

Predictor	Adjusted OR	95% CI	*P*value
Age (per 10 years)	1.32	1.08-1.62	0.007
IDH-wildtype (vs. mutant)	3.48	1.95-6.21	<0.001
Necrosis (present vs. absent)	2.32	1.39-3.87	0.001
Contrast enhancement (present vs. absent)	1.85	1.08-3.17	0.025
Edema (severe vs. none/mild)	2.45	1.32-4.55	0.004
CE-VOI (per doubling)	1.12	0.95-1.33	0.18

Model additionally adjusted for histological grade; c-statistic = 0.782.

Association between CDCA7 expression and MRI radiomic features

The radiomic subanalysis included 85 patients with high-quality tumor segmentations. Of 107 features extracted from postcontrast T1-weighted and T2-FLAIR images, 23 remained significantly correlated with continuous *CDCA7* expression after Benjamini–Hochberg correction, with absolute Spearman correlation coefficients ranging from 0.32 to 0.48 (all FDR-adjusted P<0.05). Among the strongest associations, GLCM Correlation was inversely correlated with *CDCA7* expression (ρ=-0.43), whereas GLCM Contrast (ρ=0.45) and GLSZM Large Area Emphasis (ρ=0.41) were positively correlated (all raw P<0.001; FDR-adjusted P<0.05). These findings indicate that higher *CDCA7* expression is associated with coarser texture and greater local intensity variation.

Five-feature radiomic model classified CDCA7-high and CDCA7-low tumors with an AUC of 0.76 (95% CI, 0.67–0.85) in leave-one-out cross-validation, supporting a moderate association between *CDCA7* overexpression and MRI-derived measures of tissue disorganization and tumor heterogeneity.

Co-expression and functional-enrichment analyses

LinkedOmics analysis identified broad sets of genes positively and negatively co-expressed with *CDCA7* in the TCGA glioma cohort. Gene Ontology analyses across biological process, cellular component, and molecular function categories, together with KEGG pathway analysis, demonstrated significant enrichment patterns among *CDCA7*-associated genes.

Association of CDCA7 expression with immune-cell infiltration

ssGSEA and Spearman correlation analysis demonstrated a heterogeneous immune-infiltration pattern across the 24 evaluated immune-cell populations (figure 3A). The strongest positive association was observed for T-helper 2 cells (ρ=0.681), followed by macrophages (ρ=0.267) and eosinophils (ρ=0.217). In contrast, *CDCA7* expression was negatively correlated with follicular helper T cells (ρ=-0.367), mast cells (ρ=-0.308), effector-memory T cells (ρ=-0.262), CD56bright natural killer cells (ρ=-0.261), and plasmacytoid dendritic cells (ρ=-0.258). These results indicate substantial *CDCA7*-associated remodeling of the glioma immune microenvironment, with the direction of association varying among immune-cell populations.

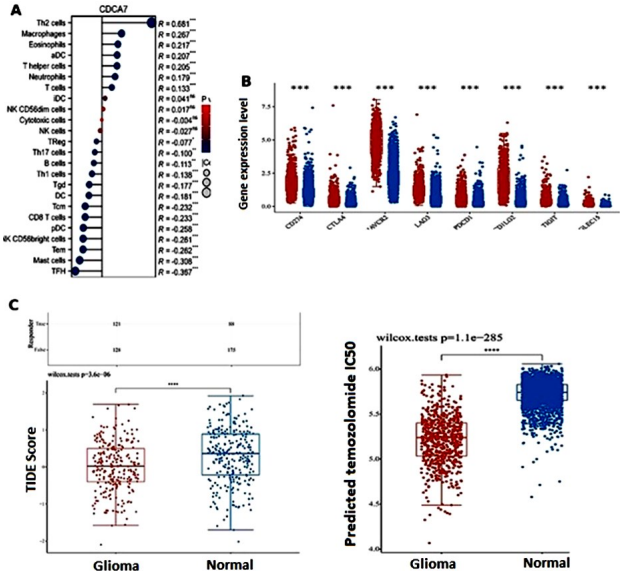


Figure 3. *CDCA7*-associated immune landscape and predicted therapeutic response. **(A)** Spearman correlations between CDCA7 expression and enrichment of 24 immune-cell populations. **(B)** Expression of the evaluated immune-checkpoint genes in glioma and normal brain tissues; the y-axis indicates gene expression level. **(C)** TIDE scores in glioma and normal tissues. **(D)** Predicted temozolomide IC50 values in glioma and normal tissues; the y-axis indicates predicted temozolomide IC50.

Immune-checkpoint expression, TIDE scores, and predicted drug sensitivity

Glioma tissues showed significantly higher expression of all evaluated immune-checkpoint genes than normal brain tissues, including *PDCD1*, *TIGIT*, *CTLA4*, *HAVCR2*, *PDCD1LG2*, *CD274*, *LAG3*, and *SIGLEC15* (Figure 3B). TIDE scores also differed significantly between glioma and normal tissues, with lower median scores in glioma tissues (figure 3C).

[Downloaded from ijrr.com on 2026-11-12]

[DOI: 10.61186/ijrr.24.4.34]

Predicted temozolomide IC50 values were significantly lower in glioma tissues than in normal tissues (figure 3D). Predicted cisplatin IC50 values were likewise lower in glioma tissues, suggesting greater predicted sensitivity to both agents.

CDCA7 knockdown suppresses glioma cell proliferation, invasion, and migration and enhances sensitivity to TMZ and CDDPCDCA7 expression was higher in four glioma cell lines (LN229, U118, U251, and T98G) than in normal HMC3 cells (Figure 4A). After 48 h of siRNA transfection, RT-qPCR showed that siRNA-CDCA7-1 had the highest knockdown efficiency (Figure 4B, C). MTS, Transwell, and wound healing assays showed that CDCA7 knockdown reduced the proliferation, invasion, and migration of U251 and T98G cells, respectively (Figure 4D–G). Since CDCA7 is associated with sensitivity to TMZ and CDDP, MTS assays were further performed and showed that the IC50 values of TMZ and CDDP were 235.1 μM and 26.71 μM, respectively (Figure S1A, B). Compared with the control group, cell viability was decreased in the siRNA-CDCA7 group and the TMZ or CDDP monotherapy groups; compared with TMZ or CDDP alone, cell viability was significantly decreased and the apoptotic proportion was significantly increased in the siRNA-CDCA7 + TMZ and siRNA-CDCA7 + CDDP groups (Figure S1A–D). These results indicate that CDCA7 knockdown suppresses glioma cell proliferation, invasion, and migration and enhances the sensitivity of U251 cells to TMZ and CDDP.

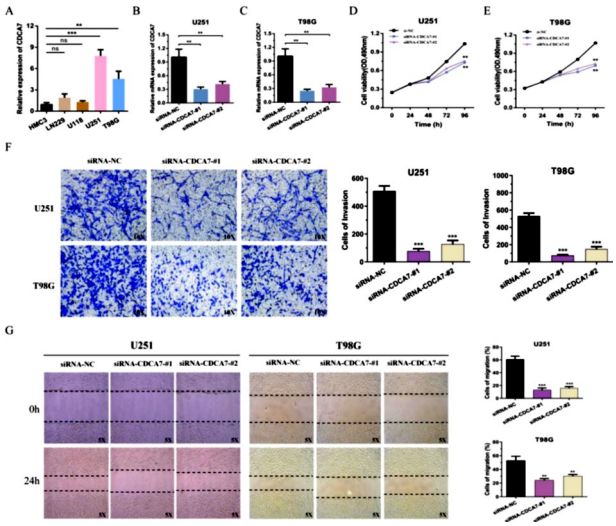


Figure 4. The deletion of CDCA7 suppressed the proliferation, invasion, and migration of U251 and T98G cells. **(A)** Expression of CDCA7 in normal and glioma cell lines. **(B, C)** Expression of CDCA7 decreased in the siRNA group in U251 and T98G cells. **(D, E)** The MTS assay revealed that si-CDCA7 transfection inhibits U251 and T98G cell proliferation. **(F, G)** Downregulation of CDCA7 reduced the invasion and migration abilities of U251 and T98G cell lines, as revealed by the transwell and scratch experiments.

DISCUSSION

The most prevalent malignant tumors of the central nervous system are gliomas. Even though glioma patients' prognosis has improved due to advancements in diagnosis and treatment, patients with advanced gliomas still have a poor prognosis. To enhance the effectiveness of immunotherapy and glioma prognosis, it is crucial to find novel molecular targets. Integrating molecular biomarkers with traditional imaging is one promising strategy to address these issues.

Diffusion-weighted imaging, perfusion imaging, and MRI with gadolinium contrast are examples of conventional imaging modalities that offer useful information about the location, size, grade, and response to treatment of tumors. Nevertheless, these methods are constrained by their limited sensitivity for detecting residual tumors following resection, their incapacity to predict molecular subtypes or immune microenvironment characteristics, and their inability to accurately differentiate true tumor progression from pseudoprogression (inflammation related to treatment) [19, 20]. Although radiomics and sophisticated imaging methods have been developed to get beyond some of these restrictions, they are still mostly experimental and non-standardized [21]. By offering details on tumor biology at the molecular level, molecular biomarkers like *CDCA7* may supplement imaging and enhance prognostic stratification and diagnostic precision.

A 371 kDa nuclear protein with 47 amino acids is encoded by *CDCA7*, a member of the cell cycle-related gene family found on chromosome 2q31 [22]. It affects the expression of a number of target genes related to apoptosis and cell cycle progression [11, 15, 23]. *CDCA7* promotes tumor growth and is often overexpressed in many malignancies [16, 24, 25]. Tumor proliferation, metastatic recurrence status, and a poor prognosis are all linked to its high upregulation in TNBC, the most aggressive subtype of breast cancer [26]. According to Wang et al., *CDCA7* was strongly expressed in lung adenocarcinoma (LUAD) and stimulated the G1 phase, which led to cell proliferation [12, 25]. *CDCA7* is essential for lymphoma cell invasion and migration. Our study is the first to show the relationship between *CDCA7* expression and immune cell infiltration, immune checkpoint regulation, and its potential as a biomarker for immune checkpoint blockade therapy in gliomas, despite the fact that *CDCA7* expression has been reported in gliomas [27, 28]. Furthermore, its potential uses are still unknown. According to the study, glioma cell lines and samples had far greater levels of *CDCA7* expression than normal samples. We discovered a correlation between *CDCA7* and immune checkpoint regulation and immune cell infiltration, suggesting that *CDCA7* may be a biomarker for predicting the response to ICB treatments. In order to create a

[Downloaded from ijrr.com on 2026-11-12]

[DOI: 10.61186/ijrr.24.4.34]

prediction histogram, we additionally examined the expression levels of *CDCA7* in gliomas along with additional clinicopathological factors. According to our initial research, *CDCA7* may be a prognostic indicator for glioma patients. The findings point to *CDCA7* as a possible therapeutic target and offer fresh perspectives on the molecular processes underlying glioma growth. To validate its mode of action, more research is required.

In neuro-oncology, the concept of integrating genetic biomarkers with imaging-often referred to as "radiogenomics" or "imaging genomics"-has garnered significant interest [29]. In order to forecast tumor biology non-invasively, radiogenomics aims to link genetic and imaging characteristics. Certain MRI characteristics have been linked to 1p/19q codeletion, *MGMT* promoter methylation, and *IDH* mutant status. It may be possible to predict *CDCA7* status and its prognostic implications based on imaging if these correlations are further strengthened by adding *CDCA7* expression profiling. By integrating molecular data and imaging results to inform therapy choices, this strategy may result in more individualized treatment regimens. Higher *CDCA7* expression was linked to coarser tumor organization and more MRI texture heterogeneity in the current study. A five-feature radiomics model demonstrated a moderate capacity to differentiate between *CDCA7*-high and *CDCA7*-low gliomas. These results are in line with earlier radiogenomic research showing that quantitative MRI texture captures molecular heterogeneity in gliomas that is biologically significant. Thirty out of fifty-four robust MRI features in a TCGA–TCIA study of glioblastoma were associated with gene-expression modules and related biological pathways; another analysis of sixty-five glioblastomas revealed that radiomic phenotypes were more closely associated with transcriptomic profiles than with copy-number changes or somatic mutations [30]. With leave-one-out cross-validated accuracies of roughly 75%–87.5%, spatially matched biopsy–MRI studies have also demonstrated that texture-based models may predict regional changes in glioma driver genes [31]. Therefore, it is possible that increased *CDCA7* expression is reflected by greater local intensity variation, coarse texture, and disorganized tumor architecture on MRI. This is supported by the positive associations of *CDCA7* expression with GLCM Contrast and GLSZM Large Area Emphasis as well as its inverse association with GLCM Correlation. Although it is less than the AUCs of 0.90–0.95 reported for an optimized MRI-based model of EGFR expression, the five-feature model's AUC of 0.76 suggests moderate discriminatory ability and is comparable to various exploratory glioma radiomics models [32]. These findings lend credence to *CDCA7*'s potential as a radiogenomic biomarker; however, prior to clinical use, external validation in larger, independent, and acquisition-harmonized cohorts is necessary.

Because of their antagonistic or pro-tumor activities, invasive immune cells are essential for the growth of tumors. We analyzed the level of immune infiltration associated with *CDCA7* for this investigation. Additionally, T cells, macrophages, and eosinophils showed a strong correlation with *CDCA7* expression, indicating that *CDCA7* may have a role in boosting antitumoral immune responses in tumor tissues. *PDCD1* (programmed cell death 1) and CTLA-4 (cytotoxic T lymphocyte-associated antigen 4) receptors are involved in the control of T-cell immunity [33]. When cancer cells evade the immune system, *PDCD1* (PD-1) and *CD274* (PD-L1) are crucial therapeutic targets. According to the current study, *CDCA7* may prevent cancer by triggering the immune system's reaction to glioma tissue tumors. It's interesting to note that the half-maximal inhibitory concentrations of temozolomide, a popular chemotherapy drug, showed a negative correlation with *CDCA7*. This suggests that glioma patients with excessive *CDCA7* release may benefit from ICB correction. It may be possible to predict the response to ICB and chemotherapy using *CDCA7*, an underprivileged conductor. These findings offer crucial information about possible targets for glioma patients' effective pain treatment. The association between *CDCA7* expression and immune infiltration implies that *CDCA7* status may be correlated with imaging biomarkers of immunological activity, such as those derived from sophisticated MRI methods or PET imaging, offering additional utility for this genetic marker.

CONCLUSION

Higher tumor grade, poor survival, and aggressive MRI characteristics such contrast enhancement, necrosis, and severe peritumoral edema are all linked to *CDCA7*'s upregulation in gliomas. Additionally, radiomic characteristics demonstrated the ability to noninvasively predict *CDCA7* expression. Additionally, *CDCA7* was linked to changes in the glioma immune milieu, and *CDCA7* knockdown prevented glioma cells from proliferating, migrating, and invading. In conclusion, these findings point to *CDCA7* as a potentially useful biomarker for glioma prognosis, imaging, and treatment. To validate its clinical utility and mechanisms, more prospective, multicenter, and in vivo studies are required.

Acknowledgement: This research received funding from the Science and Technology Research Project of the Education Department of Jiangxi Province, China (grant no. GJJ211810, GJJ2201940).

Conflict of interest: The authors report no conflicts of interest.

Ethics approval and consent to participate: The

[Downloaded from ijrr.com on 2026-11-12]

[DOI: 10.61186/ijrr.24.4.34]

Institutional Review Board (IRB) at Jiujiang University Affiliated Hospital approved this study (No. jjuhmer-a-2023-0102). The human subject trials involved in this study were conducted with the informed consent of all participants and in accordance with the Declaration of Helsinki.

***Fundings*:** This work was supported by: Jiujiang Municipal Natural Science Foundation Basic Research Program (Grant No. 2025_001386_21000_0001) and Jiangxi Provincial Natural Science Foundation General Program (Grant No. 20252BAC240547), Science and Technology Research Project of the Education Department of Jiangxi Province, China (grant no.GJJ211810, GJJ2201940).

***Author contributions*:** G.Z., wrote and revised the paper. The study was conceived and designed by X.G.; S.Y., searched and selected studies. P.Z., conducted experiments to verify. F.W., prepared the figures and tables. All authors have read and agree with the final statement.

***Data availability*:** The data that support the findings of this study are available from the corresponding author upon reasonable request.

***AI declaration*:** No AI was used in preparation of this manuscript.

REFERENCES

1. Wu L, Zhu X, Song Z, Chen D, Guo M, Liang J, *et al.* (2019) Long non -coding RNA HOXA-AS2 enhances the malignant biological behaviors in glioma by epigenetically regulating RND3 expression. *Onco Targets Ther,* ***12****: 9407-9419*.
2. Agnihotri S, Gajadhar AS, Ternamian C, Gorlia T, Diefes KL, Mischel PS, *et al.* (2012) Alkylpurine–DNA–N-glycosylase confers resistance to temozolomide in xenograft models of glioblastoma multiforme and is associated with poor survival in patients. *J Clin Invest,* ***122*** *(1): 253-266*.
3. Marinari E, Allard M, Gustave R, Widmer V, Philippin G, Merkler D, *et al.* (2020) Inflammation and lymphocyte infiltration are associated with shorter survival in patients with high-grade glioma. *Oncoimmunology,* ***9****(1): 1779990*.
4. Aldape K, Brindle KM, Chesler L, Chopra R, Gajjar A, Gilbert MR, *et al.* (2019) Challenges to curing primary brain tumors. *Nat Rev Clin Oncol,* ***16****(8): 509-520*.
5. Polivka J Jr, Polivka J, Holubec L, Kubikova T, Priban V, Hes O, *et al.* (2017) Advances in experimental targeted therapy and immunotherapy for patients with glioblastoma multiforme. *Anticancer Res,* ***37****(1): 21-33*.
6. Wang J, Qi F, Wang Z, Zhang Z, Pan N, Huai L, *et al.* (2019) A review of traditional Chinese medicine for treatment of glioblastoma. *Biosci Trends,* ***13****(6): 476-487*.
7. Bijari S, Jahanbakhshi A, Abdolmaleki P (2023) Non-invasive radiomics nomogram model for determining the low and high-grade glioma base on MRI images. *Int J Radiat Res,* ***21****(2): 275-280*.
8. Louis DN, Perry A, Wesseling P, Brat DJ, Cree IA, Figarella-Branger D, *et al.* (2021) The 2021 WHO classification of tumors of the central nervous system: a summary. *Neuro Oncol,* ***23****(8): 1231-1251*.
9. Gill RM, Gabor TV, Couzens AL, Scheid MP (2013) The MYC-associated protein CDCA7 is phosphorylated by AKT to regulate MYC-dependent apoptosis and transformation. *Mol Cell Biol,* ***33****(3): 498-513*.
10. Cai C, Peng X, Zhang Y (2021) Downregulation of cell division cycle-associated protein 7 (CDCA7) suppresses cell proliferation, arrests the cell cycle of ovarian cancer, and restrains angiogenesis by modulating enhancer of zeste homolog 2 (EZH2) expression. *Bioengineered,* ***12****(1): 7007-7019*.
11. Wang H, Ye L, Xing Z, Li H, Lv T, Liu H, *et al.* (2019) CDCA7 promotes lung adenocarcinoma proliferation via regulating the cell cycle. *Pathol Res Pract,* ***215****(11): 152559*.
12. Li H, Wang S, Li X, Weng Y, Guo D, Kong P, *et al.* (2023) CDCA7 promotes TGF-β-induced epithelial–mesenchymal transition via transcriptionally regulating Smad4/Smad7 in ESCC. *Cancer Sci,* ***114*** *(1): 91-104*.
13. Wu B, Huang Y, Luo Y, Ma A, Wu Z, Gan Y, *et al.* (2020) The diagnostic and prognostic value of the cell division cycle-associated gene family in hepatocellular carcinoma. *J Cancer,* ***11****(19): 5727-5737*.
14. Lu P, Cheng W, Fang K, Yu B (2022) Multidimensional study of cell division cycle-associated proteins with prognostic value in gastric carcinoma. *Bosn J Basic Med Sci,* ***22****(1): 64-76*.
15. Guo Y, Zhou K, Zhuang X, Li J, Shen X (2021) CDCA7-regulated inflammatory mechanism through the TLR4/NF-κB signaling pathway in stomach adenocarcinoma. *Biofactors,* ***47****(5): 865-878*.
16. Sato W, Ikeda K, Gotoh N, Inoue S, Horie K (2022) Efp promotes growth of triple-negative breast cancer cells. *Biochem Biophys Res Commun,* ***624****: 81-88*.
17. Jiménez-P R, Martín-Cortázar C, Kourani O, Chiodo Y, Cordoba R, Domínguez-Franjo MP, *et al.* (2018) CDCA7 is a critical mediator of lymphomagenesis that selectively regulates anchorage-independent growth. *Haematologica,* ***103****(10): 1669-1678*.
18. Vasaikar SV, Straub P, Wang J, Zhang B (2018) LinkedOmics: analyzing multi-omics data within and across 32 cancer types. *Nucleic Acids Res,* ***46****(D1): D956-D963*.
19. Martín-Cortázar C, Chiodo Y, Jiménez RP, Bernabé M, Cayuela ML, Iglesias T, *et al.* (2020) CDCA7 finely tunes cytoskeleton dynamics to promote lymphoma migration and invasion. *Haematologica,* ***105****(3): 730-740*.
20. Qin XY, Feng J, Chen G, Dou XW, Dai XQ, Dong HL, *et al.* (2019) ZBTB24 regulates the apoptosis of human T cells via the CDCA7/ TRAIL-receptor axis. *Biochem Biophys Res Commun,* ***514****(1): 259-265*.
21. Ye L, Li F, Song Y, Yu D, Xiong Z, Li Y, *et al.* (2018) Overexpression of CDCA7 predicts poor prognosis and induces EZH2-mediated progression of triple-negative breast cancer. *Int J Cancer,* ***143****(10): 2602-2613*.
22. Wang Y, Zhao Y, Zhang Z, Zhang J, Xu Q, Zhou X, *et al.* (2023) High expression of CDCA7 in the prognosis of glioma and its relationship with ferroptosis and immunity. *Genes (Basel),* ***14****(7): 1406*.
23. Li R, Chen Y, Yang B, Li Z, Wang S, He J, *et al.* (2024) Integrated bioinformatics analysis and experimental validation identified CDCA families as prognostic biomarkers and sensitive indicators for rapamycin treatment of glioma. *PLoS One,* ***19****(1): e0295346*.
24. Li H, Weng Y, Wang S, Wang F, Wang Y, Kong P, *et al.* (2021) CDCA7 facilitates tumor progression by directly regulating CCNA2 expression in esophageal squamous cell carcinoma. *Front Oncol,* ***11****: 734655*.
25. van der Leun AM, Thommen DS, Schumacher TN (2020) CD8+ T-cell states in human cancer: insights from single-cell analysis. *Nat Rev Cancer,* ***20****(4): 218-232*.
26. Wang Z, Su G, Dai Z, Meng M, Zhang H, Fan F, *et al.* (2021) Circadian clock genes promote glioma progression by affecting tumor immune infiltration and tumor cell proliferation. *Cell Prolif,* ***54****(3): e12988*.
27. Rowshanravan B, Halliday N, Sansom DM (2018) CTLA-4: a moving target in immunotherapy. *Blood,* ***131****(1): 58-67*.
28. Sun C, Mezzadra R, Schumacher TN (2018) Regulation and function of the PD-L1 checkpoint. *Immunity,* ***48****(3): 434-452*.
29. Begagić E, Bečulić H, Đuzić N, Džidić-Krivić A, Pugonja R, Muharemović A, *et al.* (2024) CRISPR/Cas9-mediated gene therapy for glioblastoma: a scoping review. *Biomedicines,* ***12****(1): 238*.
30. Gevaert O, Mitchell LA, Achrol AS, Xu J, Echegaray S, Steinberg GK, *et al.* (2014) Glioblastoma multiforme: exploratory radiogenomic analysis by using quantitative image features. *Radiology,* ***273****(1): 168-174*.
31. Hu LS, Ning S, Eschbacher JM, Baxter LC, Gaw N, Ranjbar S, *et al.* (2017) Radiogenomics to characterize regional genetic heterogeneity in glioblastoma. *Neuro Oncol,* ***19****(1): 128-137*.
32. Sun C, Fan L, Wang W, Wang W, Liu L, Duan W, *et al.* (2021) Radiomics and qualitative features from multiparametric MRI predict molecular subtypes in patients with lower-grade glioma. *Front Oncol,* ***11****: 756828*.
33. Alegre ML, Frauwirth KA, Thompson CB (2001) T-cell regulation by CD28 and CTLA-4. *Nat Rev Immunol,* ***1****(3): 220-228*.

[Downloaded from ijrr.com on 2026-11-12]

[DOI: 10.61186/ijrr.24.4.34]

[DOI: 10.61186/ijrr.24.4.34] [Downloaded from ijrr.com on 2026-11-12]